ORIGINAL PAPER

Speciation of tin ions in oxide glass containing iron oxide through solvent extraction and inductively coupled plasma atomic emission spectrometry after the decomposition utilizing ascorbic acid

Yoshitaka Saijo[1,3] · Makiko Murata[1] · Takato Kajihara[2] · Hiroyuki Hijiya[2] · Yuichi Suzuki[1] · Ryoji Akiyama[1] · Masahiro Shimizu[3] · Yasuhiko Shimotsuma[3] · Kiyotaka Miura[3]

Abstract

Determining the concentrations of different Sn ions in glass containing iron oxide by wet chemical analysis is a challenge because a redox reaction occurs between Sn^{2+} and Fe^{3+}. A chemical analysis method for determining the concentrations of Sn^{2+} and Sn^{4+} in soda lime glass containing iron oxide was proposed. A mixture of ascorbic acid, hydrochloric acid, and hydrofluoric acid was used to decompose the sample in a vessel with nitrogen flow. Ascorbic acid functioned as a reductant for Fe^{3+}. Subsequently, the Sn^{2+} were separated as a diethyldithiocarbamate complex. Furthermore, inductively coupled plasma atomic emission spectroscopy was used to determine the concentrations of Sn^{4+} and total Sn, from which the concentration of Sn^{2+} can be calculated. The results were validated by comparing ratios of Sn^{2+} to total Sn to results obtained using Mössbauer spectroscopy. The results were in agreement, thereby validating the use of the proposed approach.
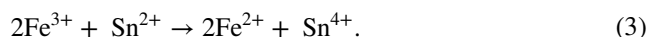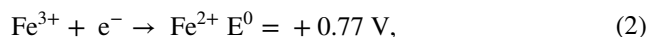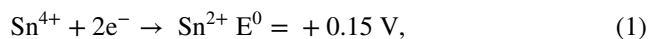
Keywords Glass · Extraction · Separation · Valence

Introduction

Glass is a versatile material used in a wide variety of industries. The incorporation of trace elements into glass can alter its color, optical, and manufacturing properties. Tin oxide is used in trace quantities as a color modifier for gold and copper ruby glass [1], a fluorescent agent [2], and a fining agent [3, 4]. These processes are based on reduction–oxidation reactions. Determining the concentrations of Sn^{2+} and Sn^{4+} in glass is important, and a reliable method is required. Methods for determining Sn valence in glass can typically be divided into wet chemical and physical analyses.

Examples of wet chemical analysis include titration [5] and spectrophotometric methods [6]. These methods can be performed daily in laboratories, and the common advantages of wet chemical analysis are better precision, lower detection limit, and lower cost [7]. However, a major drawback of wet chemical analysis of glass materials for valence speciation is the change in the valence of the target element during decomposition using hydrofluoric acid. Generally, an inert atmosphere can prevent the oxidation of species by air during sample decomposition [8–10]. The other possible valence change can be caused by the redox reaction with other multivalent elements. Fe is a multivalent element that causes the redox reaction with Sn due to the standard potential energy of the following reactions:

$$Sn^{4+} + 2e^- \rightarrow Sn^{2+}\ E^0 = +0.15\ V, \tag{1}$$

$$Fe^{3+} + e^- \rightarrow Fe^{2+}\ E^0 = +0.77\ V, \tag{2}$$

$$2Fe^{3+} + Sn^{2+} \rightarrow 2Fe^{2+} + Sn^{4+}. \tag{3}$$

Industrial glass often contains Fe either due to a deliberate addition of Fe-containing raw materials, or as an unavoidable impurity in other added raw materials [11, 12]. The previously reported methods [5, 6] are not suitable for industrially manufactured glass materials due to the redox

✉ Yoshitaka Saijo
yoshitaka.saijo@agc.com

1   Innovative Technology Laboratories, AGC Inc., 1-1 Suehiro-cho, Tsurumi-ku, Yokohama 230-0045, Japan
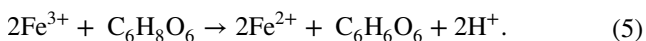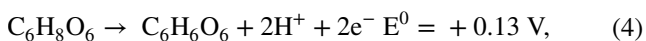
2   Materials Integration Laboratories, AGC Inc., 1-1 Suehiro-cho, Tsurumi-ku, Yokohama 230-0045, Japan

3   Department of Material Chemistry, Graduate School of Engineering, Kyoto University, Kyoto 615-8510, Japan

reaction (Eq. 3) that occurs during decomposition using hydrofluoric acid. In the previously reported methods, redox reactions were not considered [5] or iron-free glass materials synthesized in the laboratory were used [6].

Examples of physical analysis are Mössbauer spectroscopy [13–17], X-ray absorption fine structure (XAFS) [18–20], high-resolution X-ray fluorescence analysis (HR-XRF) [21, 22], and X-ray photoelectron spectroscopy (XPS) [23]. A common advantage of physical analysis is elemental selectivity as the interference from other elements, including Fe, is small or negligible. However, these methods have limitations. XAFS requires the use of synchrotron radiation facilities, and its routine use is challenging. One of the drawbacks of HR-XRF is the low signal-to-noise ratio owing to its two-crystal system. Additionally, this equipment is not widely used, and a long analysis time is required to obtain a sufficient signal-to-noise ratio for glass materials that contain trace amounts of Sn. Another drawback is that HR-XRF requires either reference materials, or a different method to determine the concentration of total Sn to obtain the concentrations of Sn^{2+} and Sn^{4+}. The drawbacks of XPS include the analysis depth and sensitivity. The analysis depth is less than 10 nm, which is too shallow to determine the Sn valence for the bulk of the sample. XPS usually requires more than 1 mass% of Sn to determine the precise valence state.

As mentioned above, both wet chemical and physical analyses have advantages and disadvantages. Wet chemical analysis is the preferred method to routinely analyze and determine the presence of Sn in glass, but faces challenges in determining the concentration of different Sn valences. Therefore, this study aims to propose, demonstrate, and validate a novel wet chemical analysis method for Sn speciation in glass containing iron oxide. The first challenge is to maintain the valence of Sn during wet analysis while preventing the redox reaction between Sn^{2+} and Fe^{3+}. There are several possible approaches: a kinetic approach that slows down the redox reaction and virtually eliminates the reaction [24], masking Fe^{3+} [25], and expelling Fe^{3+} from the system [26] before causing the redox reaction. In this study, we added a reducing agent to reduce Fe^{3+}, thereby preventing the redox reaction between Sn^{2+} and Fe^{3+}. The selected reducing agent was ascorbic acid ($C_6H_8O_6$), a well-known reducing agent for Fe^{3+} (Eqs. 4, 5). The redox reaction between ascorbic acid and Fe^{3+} occurs readily at pH 1.5 or lower and ascorbic acid does not cause any redox reaction with Sn [27].

$$C_6H_8O_6 \rightarrow C_6H_6O_6 + 2H^+ + 2e^- \quad E^0 = +0.13 \text{ V}, \quad (4)$$

$$2Fe^{3+} + C_6H_8O_6 \rightarrow 2Fe^{2+} + C_6H_6O_6 + 2H^+. \quad (5)$$

The second challenge is to separately measure the concentration of each valence of Sn, namely Sn^{2+} and Sn^{4+}. Several possible approaches exist: coloring either ion and subsequently measuring the concentration using a colorimetric method [8, 9]; separating either ion using a volatilization separation method and measuring the concentration [10]; separating each ion using a solvent extraction method. A solvent extraction method utilizing diethyldithiocarbamate (DDTC) was used since it selectively extracts Sn^{2+} to an organic phase [28] at pH values ranging from 1 to 2.2 [29]. Considering the above two points, a mixture of ascorbic acid, hydrofluoric acid, and hydrochloric acid, which was adjusted to a suitable pH, was used to decompose the glass samples, prevent the redox reaction between Sn^{2+} and Fe^{3+} and separate Sn^{2+} and Sn^{4+} by the solvent extraction method using DDTC. The concentrations of Sn in the glass samples were found to be too low to be determined by the colorimetry method [28]; therefore, inductively coupled plasma atomic emission spectrometry (ICP-AES) was used to determine Sn^{4+} and total Sn in the liquid phase. Sn^{2+} was calculated by subtracting Sn^{4+} from the total Sn concentration. The proposed method was validated by comparing the average concentration of Sn valences obtained by Mössbauer spectroscopy for the prepared soda lime glass materials doped with tin oxide and iron oxide.

Experimental

Material preparation

The glass studied had the following standard soda lime glass mass% composition: $16.5Na_2O \cdot 9.4CaO \cdot 74.1SiO_2$. They were produced by melting from raw materials of Na_2CO_3, $CaCO_3$, and SiO_2 and doped with 0.5 mass% SnO_2, 0–0.05 mass% Fe_2O_3, and 0–0.5 mass% carbon, as a reducing reagent, using a platinum crucible at 1500 °C. Table 1 lists the sample names and dopant concentrations used. The samples were then cut and mirror-polished using cerium oxide. A glass standard reference material, SRM 1830 (National Institute of Standards and Technology, Gaithersburg, USA), was used to confirm the effect of Fe^{3+}. Table S1 (Supporting Information) lists the certified compositions. The concentration of Fe^{3+} in SRM 1830 was calculated from the certified composition of total Fe and Fe^{2+}.

Table 1 Sample names and the concentrations of dopants used given in mass%

Sample name	SLS-M01	SLS-M02	SLS-M03	SLS-M04
SnO_2	0.50	0.50	0.50	0.50
Fe_2O_3	–	0.05	–	0.05
C	–	–	0.50	0.50

Apparatus and instrumentation

A wavelength-dispersive X-ray fluorescence spectrometer (ZSX Primus II, Rigaku Corporation, Tokyo, Japan) was used to measure the compositions of produced samples. A 120 mL polytetrafluoroethylene (PTFE) decomposition vessel was used to decompose the glass samples with reagents. A magnetic stirrer and a 40×7 mm^2 stirring bar were used to stir the samples and reagents in the vessel. A 100 mL polypropylene separatory funnel with a stop valve was used to add reagents to the vessel. A 100 mL glass separatory funnel was used to extract Sn^{2+} into the organic phase. A 50 mL volumetric flask was used to fill the sample solutions. A 10 mL syringe (Terumo Corporation, Tokyo, Japan) and a syringe filter with 0.45 μm pore (Toyo Roshi Kaisya, Ltd., Tokyo, Japan) were used to transfer sample solutions and to remove any unexpected solids. An inductively coupled plasma atomic emission spectrometer (SPS5520, Hitachi High-Tech Corporation, Tokyo, Japan) was used to determine the Sn concentration.

Reagents and chemicals

Hydrofluoric acid (HF, 50 mass%), hydrochloric acid (HCl, 36 mass%) of atomic absorption spectrometry grade, boric acid ascorbic acid, mixed xylene (Kanto Chemical Co., Inc., Tokyo, Japan) of special grade, and diethylammonium diethyldithiocarbamate (FUJIFILM Wako Pure Chemical Corporation, Osaka, Japan) of Wako 1st grade were used. Standard solutions of Sn and Fe (1 g/L) of ion chromatography grade (Kanto Chemical Co., Inc., Tokyo, Japan) were used. Deionized water was degassed and used.

Composition analysis

The compositions of produced samples were measured by XRF using fundamental parameter procedures [30]. The X-ray tube for primary excitation was a rhodium anode X-ray tube with the exciting conditions of 50 kV and 60 mA, operated under vacuum conditions. The measurement area was 30mmφ. The SnO$_2$ concentrations of samples were determined by chemical analysis, as was done for the total Sn in this study. Details were presented in the next two sections.

Decomposition of glass samples and the separation of Sn^{2+}

Figure 1 shows the apparatus used for the decomposition of the glass samples. A 30 mg aliquot of the ground glass was accurately weighed in a PTFE decomposition vessel and moistened with 1 mL of 5 mass% ascorbic acid. A mixture of 10 mL of 1.4 mol/L HF and 0.12 mol/L HCl was added to the polypropylene separatory funnel on the vessel, which
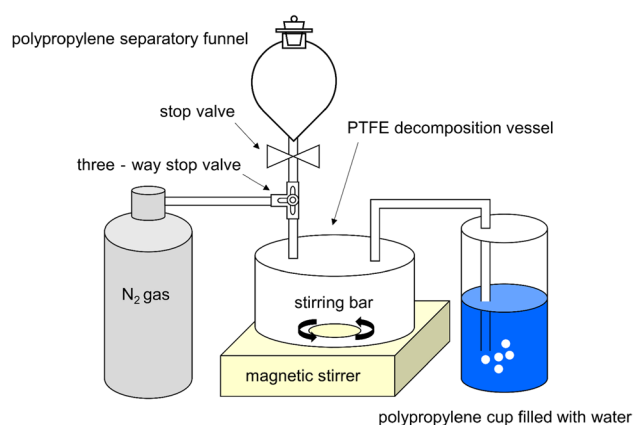
Fig. 1 Schematic representation of the experimental setup for decomposition of the glass samples. Glass samples are decomposed in the PTFE decomposition vessel with nitrogen flow. The nitrogen flow in the vessel is confirmed by the presence of nitrogen bubbles in a polypropylene cup filled with water

was degassed by passing nitrogen through the solution for 2 min. This was done by twisting the stop valve and the three-way valve to expel oxygen in the solution. The decomposition vessel was purged by passing nitrogen through at approximately 10 mL/s for 5 min to remove oxygen in the solution. The degassing process and purging process are collectively named 'deoxidizing process'. The mixture of HF and HCl solution was added to the decomposition vessel by twisting the stop valve and the three-way stop valve. Glass samples were decomposed by stirring for 30 min with nitrogen flow at approximately 10 mL/s. A boric acid solution (10 mL, 4 mass%) was added to the polypropylene separatory funnel during decomposition. After decomposition, nitrogen gas was passed through the boric acid solution in the funnel for 2 min by twisting the stop valve and the three-way valve to expel oxygen in the solution. The solution was added to the decomposition vessel and stirred with the decomposition solution for 1 min to ensure safety; boric acid complexes with free HF to produce HBF$_4$ [31], and the solution does not substantially dissolve glassware [32, 33]. The vessel was opened, and the solution in the vessel was transferred to a 50 mL volumetric flask. A small amount of water was added to the vessel to wash it; the water was transferred to the same 50 mL volumetric flask, and the solution was diluted to 50 mL with water. The solution in the flask was named "solution A." Approximately 10 mL of solution A was sampled twice using a syringe. The 20 mL solution A sample was added with a syringe into a 100 mL glass separatory funnel containing 5 mL of xylene mixed with 0.1 mass% diethylammonium diethyldithiocarbamate. A syringe filter was used to remove any unexpected solids. The funnel was shaken for 1 min to extract Sn^{2+} in solution A into the organic phase. This procedure was performed

twice. The water phase in the funnel was sampled, and the solution was named "solution B." These procedures were performed three times ($n = 3$) for each sample.

Determination of Sn

The concentrations of Sn present in solutions A and B, which contain total Sn and Sn^{4+}, respectively, were determined by ICP-AES. Table 2 lists the measurement conditions of ICP-AES. The concentrations of total Sn, Sn^{4+}, and Sn^{2+} in the glass samples were calculated as follows:

In mass%

Total Sn $\left(\text{as SnO}_2 \text{ mass}\% \right)$

$$= \frac{\text{Sn in solution A} \left(\frac{\mu g}{mL} \right) \times 50 (mL)}{\text{Sample weight (mg)}} \times 10^{-1} \times 1.2696, \quad (6)$$

$Sn^{4+} \left(\text{as SnO}_2 \text{ mass}\% \right)$

$$= \frac{\text{Sn in solution B} (\mu g/mL) \times 50 (mL)}{\text{Sample weight (mg)}} \times 10^{-1} \times 1.2696, \quad (7)$$

$Sn^{2+} \left(\text{as SnO}_2 \text{ mass}\% \right)$

$$= \text{Total Sn} \left(\text{as SnO}_2 \text{mass}\% \right) - Sn^{4+} \left(\text{as SnO}_2 \text{mass}\% \right). \quad (8)$$

In mmol/g

Total Sn (as Sn mmol/g)

$$= \frac{\text{Sn in solution A} \left(\frac{\mu g}{mL} \right) \times 50 (mL)}{\text{Sample weight (mg)}} \times 10^2 \div 118.71 (g/mol), \quad (9)$$

Sn^{4+} (as Sn mmol/g)

$$= \frac{\text{Sn in solution B} (\mu g/mL) \times 50 (mL)}{\text{Sample weight (mg)}} \times 10^2 \div 118.71 (g/mol), \quad (10)$$

Sn^{2+} (as Sn mmol/g)

$$= \text{Total Sn (as Sn mmol/g)} - Sn^{4+} (\text{as Sn mmol/g}). \quad (11)$$

The concentrations were calculated as SnO_2 mass% following the conventions for describing the composition of oxide glass, and as Sn mmol/g to calculate the redox reaction between Sn^{2+} and Fe^{3+}. Equations 6 and 7 show the conversion factor, 1.2696, from Sn to SnO_2. Equations 9 and 10 show the atomic weight of Sn, 118.71 g/mol. In this study, the ratio of Sn^{2+} to total Sn is defined as the Sn redox, indicating the degree of reduction, as follows:

$$\text{Sn redox (\%)} = \frac{Sn^{2+} \left(\text{as SnO}_2 \text{ mass}\% \right)}{\text{Total Sn} \left(\text{as SnO}_2 \text{ mass}\% \right)} = \frac{Sn^{2+} (\text{as Sn mmol/g})}{\text{Total Sn} (\text{as Sn mmol/g})}. \quad (12)$$

Blank test

A blank test was conducted throughout the entire procedure, consisting of the decomposition, separation, and determination procedures. The test was repeated four times to calculate the mean blank value and the standard deviation (σ). The limit of detection was defined as the mean blank value plus 3σ. The limit of quantification was defined as the mean blank value plus 10σ.

The effects of Fe^{3+}

The effect of Fe^{3+} on the proposed method was also investigated. A 30 mg aliquot of ground SRM 1830 was added before 30 mg of SLS-M03 was decomposed to confirm the effect of Fe^{3+} in SRM 1830 on the obtained Sn redox value. Because SRM 1830 contains Fe^{3+}, if the redox reaction between Fe^{3+} in SRM 1830 and Sn^{2+} in SLS-M03 occurs (Eq. 3), the obtained Sn redox value decreases as compared to that of SLS-M03. If the proposed method can prevent the redox reaction (Eq. 3), the obtained Sn redox value would be the same as that of SLS-M03. The test was repeated twice ($n = 2$).

Various amounts of Fe^{3+} (0.12 mol% HCl solution), ranging from 0.42 to 8.4 μmol, were added before 30 mg SLS-M03 was decomposed. Ascorbic acid was not added to the iron containing solution, preventing Fe^{3+} to be reduced to Fe^{2+}, to confirm the effect of Fe^{3+}. Other conditions were kept the same as those described in Section 'Decomposition of glass samples and the separation of Sn^{2+}'.

The effects of addition of ascorbic acid, and the deoxidizing process

To validate the proposed method, the effects of addition of ascorbic acid, and the deoxidizing process were tested using sample SLS-M04. The tests were performed with and without the addition of ascorbic acid, each scenario tested in combination with and without the deoxidizing process. Other

Table 2 ICP-AES measurement conditions

RF power	1.2 kW
Plasma gas flow	15.0 L/min
Auxiliary gas flow	1.5 L/min
Nebulizer gas pressure	0.75 MPa
Emission line	Sn (II): 189.927 nm

conditions were kept the same as those described in Section 'Decomposition of glass samples and the separation of Sn^{2+}'.

Mössbauer spectroscopy measurement

The valence states of Sn in the glass samples were measured by ^{119}Sn spectroscopy using standard transmission geometry. Gamma rays (γ-rays) emitted from $Ca^{119m}SnO_3$ were used. The Doppler velocity range of the source was ± 8 mm/s. The velocity scale was calibrated using a ^{57}CoRh source and a standard α-Fe foil absorber. The velocity 0 mm/s criterion was set to the peak position of the $CaSnO_3$ (Sn^{4+}) standard material. A Pd 50 μm foil was used as a filter to cut the interfering Sn-Kα X-rays emitted from the Sn source. A NaI scintillation counter was used for γ-ray detection. The source activity was 444–416 MBq (12.0–11.2 mCi). The ^{119}Sn Mössbauer spectra at room temperature were measured for all glass samples in plate form. The Mössbauer spectra of ^{119}Sn of a sample material doped with 0.5 mass% SnO_2 and 0.5 mass% carbon were measured in a flow-type cryostat at four temperatures (78 K, 100 K, 200 K, and 300 K). The obtained spectra were deconvoluted using Lorentzian curves. For the oxidized atmosphere samples (SLS-M01, SLS-M02), the spectra were deconvoluted using one set of quadrupole-split doublet corresponding to Sn^{4+}, and one set of quadrupole-split doublet corresponding to Sn^{2+}. For the reduced atmosphere samples (SLS-M03, SLS-M04), the spectra were deconvoluted using one set of quadrupole-split doublet corresponding to Sn^{4+} and two sets of quadrupole-split doublet corresponding to Sn^{2+}. The Debye temperature of the Sn^{2+} and Sn^{4+} sites were obtained from the slope of the straight line in the relationship between the temperature and the logarithm of the integral absorption intensities for the sample material doped with 0.5 mass% SnO_2 and 0.5 mass% carbon, by applying the high-temperature approximation formula of the Debye model:

$$\ln f = -\frac{6E_R}{k_B \theta_D^2} \times T, \tag{13}$$

$$E_R = \frac{E_\gamma^2}{2Mc^2}, \tag{14}$$

$$A = \text{const} \times f. \tag{15}$$

Here, f represents the recoilless fraction, θ_D is the Debye temperature of the Mössbauer ion, E_R is the recoil energy, k_B is the Boltzmann constant, T is the measurement temperature, E_γ is the energy of Mössbauer γ-rays (23.87 keV), M is the mass of the recoil nucleus ($M(Sn) = 118.90331$ u), c is the velocity of light, and A is the integral absorption intensity. Assuming the Debye temperature obtained for the sample material doped with 0.5% mass% SnO_2 and 0.5 mass% carbon is the same for all samples, the integral absorption intensities obtained for each sample at room temperature were corrected by the recoilless fraction to obtain the atomic presence ratios of Sn^{2+} and Sn^{4+}.

Results and discussion

Sample composition

Table 3 lists composition of each sample determined by XRF and chemical analysis. The compositions were close to the target values except for SnO_2. In all the samples, the concentrations of total Sn were lower than the doped concentrations (0.5 mass%). It is highly possible that Sn volatilized as SnO during melting. A small amount of Al_2O_3 was found as a result of impurities from the raw materials or the experimental environment.

Detection limit and quantification limit of the proposed method

The mean blank value, detection limit, and quantification limit of the three Sn valences are the following: for Sn^{4+}, < 0.0001, < 0.0001, and 0.004 mass%; for total Sn, < 0.0001, 0.001, and 0.003 mass%; for Sn^{2+}, 0.001, 0.002, and 0.004 mass%.

Determination of Sn^{2+} and Sn^{4+} in glass samples by the proposed method

Table 4 lists the concentrations of total Sn, Sn^{4+}, and Sn^{2+} in glass samples in the form of tin dioxides. It also lists the Sn redox, indicating the degree of reduction as the ratio of Sn^{2+} to total Sn. The repeatability of $n = 3$ was good. The Sn

Table 3 Composition of each glass sample measured by XRF and chemical analysis (given in mass%)

	SLS-M01	SLS-M02	SLS-M03	SLS-M04
SiO_2	73.6	73.6	73.6	73.6
Al_2O_3	0.10	0.11	0.13	0.12
Na_2O	16.4	16.4	16.4	16.4
CaO	9.33	9.31	9.33	9.33
SnO_2	0.40	0.40	0.33	0.34
Fe_2O_3	0.02	0.06	0.02	0.07

redox values of SLS-M03 and SLS04 were higher than those of SLS-M01 and SLS-M02, reflecting the melting conditions. SLS-M03 and SLS-M04 were produced by melting with carbon; on the other hand, SLS-M01 and SLS-M02 were produced by melting without carbon. Table 5 lists the average concentrations of total Sn, Sn^{4+} and Sn^{2+} in glass samples in form of mmol/g as well.

Effect of Fe^{3+}

The Sn redox results of SLS-M03 decomposed with SRM 1830 for $n=1$ and $n=2$ were both 74%. The concentration of Fe^{3+} in SRM 1830, calculated from the certified values of total Fe and Fe^{2+}, was 1.07 mmol/g. The concentration of total Sn and Sn^{2+} in SLS-M03 was 2.21 and 1.63 mmol/g, respectively. Thus, the Sn redox should decrease by 24% if the redox reaction between Fe^{3+} in SRM 1830 and Sn^{2+} in SLS-M03 occurs (Eq. 3). The resulting Sn redox of SLS-M03 decomposed with SRM 1830, which is equal to the Sn redox of SLS-M03, as shown in Table 4, indicating that the proposed method fully prevented the redox reaction between Sn^{2+} and Fe^{3+} during decomposition. The ascorbic acid completely reduced Fe^{3+} in SRM 1830. This is because the reaction between ascorbic acid and Fe^{3+} occurs readily [27].

Table 6 shows the Sn redox of SLS-M03 solution with added Fe^{3+} with and without the addition of ascorbic acid. It also shows the Sn redox with the standard condition in Table 4 as reference. When Fe^{3+} was added without the addition of ascorbic acid, the Sn redox decreased. This indicates that the reaction of Eq. 3 occurred during decomposition, as

Table 4 Concentrations of total Sn, Sn^{4+} and Sn^{2+} in the glass samples given in mass% of tin dioxides, as well as the calculated Sn redox

		Total Sn (as SnO_2 mass%)	Sn^{4+} (as SnO_2 mass%)	Sn^{2+} (as SnO_2 mass%)	Sn redox (%)
SLS-M01	$n=1$	0.406	0.367	0.039	9.6
	$n=2$	0.391	0.351	0.040	10
	$n=3$	0.404	0.366	0.038	9.4
	Avg	0.400	0.361	0.039	9.8
SLS-M02	$n=1$	0.403	0.382	0.021	5.2
	$n=2$	0.390	0.368	0.022	5.6
	$n=3$	0.416	0.392	0.024	5.8
	Avg	0.403	0.381	0.022	5.5
SLS-M03	$n=1$	0.317	0.090	0.227	72
	$n=2$	0.350	0.086	0.264	75
	$n=3$	0.333	0.085	0.248	74
	Avg	0.334	0.088	0.246	74
SLS-M04	$n=1$	0.333	0.080	0.253	76
	$n=2$	0.344	0.084	0.260	76
	$n=3$	0.341	0.086	0.255	75
	Avg	0.339	0.083	0.256	76

Table 5 Concentrations of total Sn, Sn^{4+}, and Sn^{2+} in the glass samples given in mmol/g

	Total Sn (mmol/g)	Sn^{4+} (mmol/g)	Sn^{2+} (mmol/g)
SLS-M01	2.66	2.40	0.26
SLS-M02	2.67	2.52	0.15
SLS-M03	2.21	0.58	1.63
SLS-M04	2.25	0.55	1.70

expected. Conversely, the Sn redox did not decrease quantitatively with respect to the amount of Fe^{3+} added. It is highly possible that the reaction rate of Eq. 3 is relatively slow and does not proceed to completion during the reaction time of this experimental condition.

The effects of addition of ascorbic acid, the deoxidizing process

Table 7 shows the Sn redox of SLS M-04 with and without the addition of ascorbic acid, with and without the deoxidizing process. It also shows the Sn redox with the standard condition in Table 4 as reference. Under the conditions where ascorbic acid was added, and the deoxidizing process was not employed, the Sn redox was lower than the standard condition. It is considered that the dissolved oxygen in the solution caused the oxidation of Sn^{2+}. From the above results, it was found that ascorbic acid acts as a reducing agent for Fe^{3+}, counteracts the redox reaction between Fe^{3+} and Sn^{2+}, and prevents the oxidation of Sn^{2+} by dissolved oxygen.

Valence analysis result by Mössbauer spectroscopy

Table 8 lists the Sn redox measured by Mössbauer spectroscopy corrected with the recoilless fractions at room temperature (300 K). The Mössbauer spectra of the glass samples at room temperature (300 K) is shown in Figure S1 (Supporting Information). Two absorption doublets were observed to be centered at isomer shifts of ~ 0 and 2.8 mm/s. The absorption at ~ 0 mm/s can be attributed to Sn^{4+} and that at ~ 2.8 mm/s to Sn^{2+}, according to previous reports [34–36]. The spectra of SLS-M03 and SLS04, where 0.5mass% carbon was added, show obvious Sn^{2+} peaks. Because the peaks of the two sets of Sn^{2+} doublets were connected continuously, it was difficult to deconvolute uniquely. However, it was confirmed that the total Sn^{2+} ratio did not depend on the deconvolution method. The Mössbauer spectra of SLS-M03 at several temperatures is shown in Figure S2 (Supporting Information). The lower the measurement temperature, the larger is the Sn^{2+} peak. Figure S3 (Supporting Information) shows the relationship between the logarithm of the integrated absorption intensity

Table 6 Sn redox of SLS-M03 with Fe^{3+} added in various amounts

Addition of ascorbic acid	Yes	No	No	No	No	No
Fe^{3+} (μmol)	0	0	0.42	0.84	1.68	8.42
Fe^{3+} mol ratio to Sn^{2+}	0	0	1	2	4	20
Sn redox of SLS-M03(%)	75[a]	68	55	56	50	< 2

[a]Standard condition

Table 7 Sn redox of SLS M-04 calculated with and without the addition of ascorbic acid, with and without degassing/N_2 purging

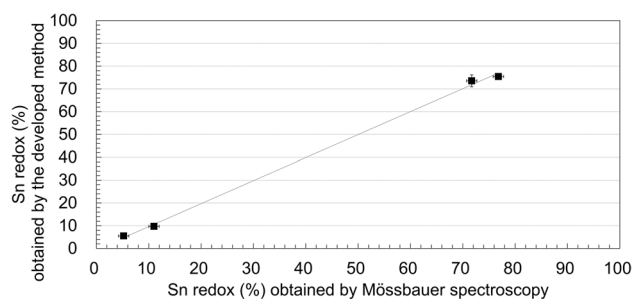| Addition of ascorbic acid	Yes	Yes	No	No
Addition of the deoxidizing process	Yes	No	Yes	No
Sn redox of SLS M-04(%)	75[a]	60	63	44

[a]Standard condition

Table 8 Sn redox measured by Mössbauer spectroscopy corrected with the recoilless fraction at room temperature (300 K)

	Sn redox (%)
SLS-M01	11
SLS-M02	5.2
SLS-M03	73
SLS-M04	77

Fig. 2 Comparison of the Sn redox obtained by Mössbauer spectroscopy and the proposed method. The values measured by Mössbauer spectroscopy were corrected with the recoilless fractions at room temperature (300 K)

of the Mössbauer spectra of Sn^{2+} and Sn^{4+} of SLS-M03 and the measurement temperatures. The calculated Debye temperatures were 185 and 266 K for Sn^{2+} and Sn^{4+}, respectively. These results are in good agreement with those of previously researched soda lime silicate glass [16, 17]. The recoilless fractions for Sn^{2+} and Sn^{4+} of SLS-M03 at each temperature calculated from the Debye temperature are listed in Table S2 (Supporting Information).

Comparison of the results of the proposed method with Mössbauer spectroscopy

Figure 2 shows a comparison of the Sn redox obtained through Mössbauer spectroscopy and the proposed method. The error bar of the *x*-axis is 2% for Mössbauer spectroscopy, and the error bar of the *y*-axis is 1 σ for the proposed method. The results were in good agreement, including the results of the samples containing iron oxide. This confirms that the proposed method determines the Sn redox accurately.

Conclusions

The present study investigates a novel wet chemical analysis method for determining the concentrations of trace total Sn and Sn^{4+} in oxide glass materials containing iron oxide. The method entails decomposing a glass sample, separating, and determining Sn^{4+} and total Sn concentrations. Sn^{2+} was calculated using total Sn and Sn^{4+}. The ratio of Sn^{2+} to total Sn (the Sn redox) were calculated. Glass samples were decomposed in a decomposition vessel with a mixture of ascorbic acid, hydrochloric acid, and hydrofluoric acid under a nitrogen purge. Ascorbic acid performed as a reducing agent for Fe^{3+}. Additionally, ascorbic acid inhibited the oxidation of Sn^{2+} by dissolved oxygen. Sn^{2+} was separated from the glass-decomposed solution into the organic phase as a diethyldithiocarbamate complex. ICP-AES was used to determine the concentrations of Sn^{4+} and total Sn. As sample materials, soda lime glasses were doped with tin oxide and iron oxide. The Sn redox were compared to those obtained using Mössbauer spectroscopy, and were found to be in excellent agreement. Thus, the proposed approach holds significant promise for routine analytical studies of glass materials without the drawbacks associated with the industry's current standard methodologies.

References

1. S.D. Stookey, J. Am. Ceram. Soc. **32**, 246 (1949). https://doi.org/10.1111/j.1151-2916.1949.tb18957.x

2. L. Skuja, J. Non Cryst. Solids. **149**, 77 (1992). https://doi.org/10.1016/0022-3093(92)90056-P

3. K. Kim, J. Am. Ceram. Soc. **96**, 781 (2013). https://doi.org/10.1111/jace.12188

4. A. Ellison, I.A. Cornejo, Int. J. Appl. Glass. Sci. **1**, 87 (2010). https://doi.org/10.1111/j.2041-1294.2010.00009.x

5. J.S. Sieger, J. Non Cryst. Solids. **19**, 213 (1975). https://doi.org/10.1016/0022-3093(75)90086-1

6. R. Pyare, P. Nath, Analyst **110**, 1321 (1985). https://doi.org/10.1039/AN9851001321

7. J.E. Amonette, J. Matyáš, Anal. Chim. Acta **910**, 25 (2016). https://doi.org/10.1016/j.aca.2015.12.024

8. D.R.J. Jones, W.C. Ansheski, D.S. Goldman, Anal. Chem. **53**, 923 (1981). https://doi.org/10.1021/ac00229a049

9. R. Akiyama, N. Kanno, Y. Suzuki, K. Yamamoto, Glass Technol. Part A. **56**, 37 (2015). https://doi.org/10.13036/17533546.56.2.37

10. Y. Saijo, Y. Suzuki, M. Murata, R. Akiyama, M. Shimizu, Y. Shimotsuma, K. Miura, J. Non Cryst. Solids. **571**, 121072 (2021). https://doi.org/10.1016/j.jnoncrysol.2021.121072

11. Y. Arai, M. Inoue, K. Ishikawa, T. Yokote, Y. Kondo, K. Mori, in *Proceedings of SID Symposium Digest of Technical Papers*, vol. 1663 (2017). https://doi.org/10.1002/sdtp.11964.

12. H. Hijiya, New Glass **34**, 14 (2019)

13. H. Masai, Y. Suzuki, T. Yanagida, K. Mibu, Bull. Chem. Soc. Jpn. **88**, 1047 (2015). https://doi.org/10.1246/bcsj.20150145

14. D. Benne, C. Rüssel, M. Menzel, K.D. Becker, J. Non Cryst. Solids. **337**, 232 (2004). https://doi.org/10.1016/j.jnoncrysol.2004.04.017

15. J.A. Johnson, C.E. Johnson, K.F.E. Williams, D. Holland, M.M. Karim, Hyperfine Interact. **95**, 41 (1995). https://doi.org/10.1007/BF02146304

16. K. Williams, C. Johnson, B. Tilley, D. Gelder, J. Johnson, J. Non Cryst. Solids. **211**, 164 (1997). https://doi.org/10.1016/S0022-3093(96)00636-9

17. K.F.E. Williams, C.E. Johnson, O. Nikolov, M.F. Thomas, J.A. Johnson, J. Greengrass, J. Non Cryst. Solids. **242**, 183 (1998). https://doi.org/10.1016/S0022-3093(98)00799-6

18. H. Masai, T. Ina, S. Okumura, K. Mibu, Sci. Rep. **8**, 415 (2018). https://doi.org/10.1038/s41598-017-18847-0

19. A.M. Flank, P. Lagarde, J. Jupille, H. Montigaud, J. Non Cryst. Solids. **357**, 3200 (2011). https://doi.org/10.1016/j.jnoncrysol.2011.03.046

20. M. Zheng, H. Wang, T. Haizheng, H. Yourong, J. Hong, J. Non Cryst. Solids. **383**, 71 (2014). https://doi.org/10.1016/j.jnoncrysol.2013.04.027

21. Y. Gohshi, O. Hirao, I. Suzuki, Adv. X-ray Anal. **18**, 406 (1974). https://doi.org/10.1154/S0376030800006911

22. H. Masuda, Y. Fukumoto, K. Morinaga, in *Engineering Sciences Reports, Kyushu University*, vol. 14, p. 173 (1992). https://doi.org/10.15017/17267

23. L. Jie, J. Non Cryst. Solids. **119**, 37 (1990). https://doi.org/10.1016/0022-3093(90)90238-H

24. N. Kanno, M. Nakase, M. Harigai, Y. Saijo, R. Akiyama, K. Takeshita, in *Abstract of the 35th Symposium on Ion Exchange & The 40th Symposium on Solvent Extraction*, Kitakyusyu, Japan, vol. 82 (2021)

25. O. Corumluoglu, E. Guadagnino, Glass Technol. **40**, 24 (1999)

26. A. Frankenberger, R.R. Brooks, M. Hoashi, Anal. Chim. Acta **246**, 359 (1991). https://doi.org/10.1016/S0003-2670(00)80973-3

27. K. Mikami, Bunseki Kagaku **27**, 160 (1978). https://doi.org/10.2116/bunsekikagaku.27.3_160

28. P.F. Wyattf, Analyst **80**, 368 (1955)

29. H. Goto, Y. Kakita, J. Jpn. Inst. Met. Mater. **20**, 319 (1956). https://doi.org/10.2320/jinstmet1952.20.6_319

30. P.J. Potts, *A handbook of silicate rock analysis, Chap. 8* (Blackie, Glasgow, 1987)

31. P.J. Potts, *A handbook of silicate rock analysis, Chap. 2* (Blackie, Glasgow, 1987)

32. B. Bernas, Anal. Chem. **40**, 1682 (1968). https://doi.org/10.1021/ac60267a017

33. D.E. Buckley, R.E. Cranston, Chem. Geol. **7**, 273 (1971). https://doi.org/10.1016/0009-2541(71)90012-X

34. G.S. Collins, T. Kachnowski, N. Benczer-Koller, M. Pasternak, Phys. Rev. B **19**, 1369 (1979). https://doi.org/10.1103/PhysRevB.19.1369

35. N. Kikuchi, A. Samizo, S. Ikeda, Y. Aiura, K. Mibu, K. Nishio, Phys. Rev. Mater. **1**, 021601 (2017). https://doi.org/10.1103/PhysRevMaterials.1.021601

36. S. Miyasaka, T. Ishiyama, M. Nakano, K. Yanagihara, Y. Hayashi, T. Omata, Appl. Surf. Sci. **532**, 147421 (2020). https://doi.org/10.1016/j.apsusc.2020.147421